Positron trapping at defects in copper oxide superconductors

T. McMullen, P. Jena, S. N. Khanna, and Yi Li
Physics Department, Virginia Commonwealth University, Richmond, Virginia 23284-2000

Kjeld O. Jensen
School of Physics, University of East Anglia, Norwich NR4 7TJ, United Kingdom
(Received 13 July 1990; revised manuscript received 2 January 1991)

Positron states and lifetimes at defects in the copper oxide superconductors $La_{2-x}Sr_xCuO_4$, $YBa_2Cu_3O_{7-x}$, and $Bi_2Sr_2CaCu_2O_{8+x}$ are calculated with use of the superposed-atom model. In the $Bi_2Sr_2CaCu_2O_{8+x}$ compound, we find that the smaller metal-ion vacancies appear to only bind positrons weakly, while missing oxygens do not trap positrons. In contrast, metal-ion vacancies in $La_{2-x}Sr_xCuO_4$ and $YBa_2Cu_3O_{7-x}$ bind positrons by ~ 1 eV, and oxygen-related defects appear to be the weak-binding sites in these materials. The sites that bind positrons only weakly, by energies $\sim k_BT$, are of particular interest in view of the complex temperature dependences of the annihilation characteristics that are observed in these materials.

I. INTRODUCTION

The copper oxide superconductors are structurally complex materials. Their parent insulators are somewhat simpler but are nonsuperconducting. To produce the metallic phases that become superconducting, the parent compounds must be doped, possibly with impurities, as in $La_{2-x}Sr_xCuO_4$ (La 2:1:4), or sometimes by changing the stoichiometry, as in $YBa_2Cu_3O_{7-x}$ (Y 1:2:3), and $Bi_2Sr_2CaCu_2O_{8+x}$ (Bi 2:2:1:2). Some of the defects have low mobility, while some, such as oxygen in Y 1:2:3, diffuse readily, and defect-free crystals are not easily produced by, for example, the annealing processes used for conventional metals. In fact, maximally defect-free samples of the oxide superconductors, which have well-characterized residual defects of known concentration, are not yet available. If such samples could be produced, they would certainly be helpful in establishing the still-mysterious mechanism of superconductivity in these materials.

Such samples would probably not be particularly useful in applications, however. More likely materials are the granular ceramics and thin films, and the junctions that will be used in devices. Some defects, such as those responsible for flux pinning, add useful properties to the materials.

As a consequence of both the unavoidability and desirability of defects in the oxide superconductors, studies of these defects are important. There are several atomic-scale probes that are sensitive to defects, and the positron is one of these probes. Positron annihilation is a well-established technique for studying defects in metals and is becoming useful in similar studies of other materials.[1,2] Methods for the calculation of positron states and annihilation characteristics for defect-trapped positrons have been developed,[3-5,1] and the procedures work extremely well for metals, where most of the emphasis has been placed. The agreement between calculated lifetimes and the measured values for the defect-trapped positrons is often only a few ps, and the trapping and the annihilation characteristics of positrons at defects in metals seems to be be quantitatively understood. A similar understanding of these processes in semiconductors and insulators is evolving.[6-11] Nevertheless, positron studies of such complex, unusual, and poorly understood new materials seemed intimidating, and were primarily driven by the unexpected apparent sensitivity of positrons to superconductivity in these materials.[12-16] At present, much of the experimental work is directed toward establishing whether or not a Fermi surface exists within the bulk materials, and this requires the positrons to be in untrapped, delocalized, Bloch states.

In addition to the temperature dependence of annihilation parameters that may be associated with superconductivity, complex temperature dependences are observed that may be, at least in part, due to thermal detrapping from weakly bound positron states.[17,16] The observed annihilation characteristics are also sample dependent, further supporting the view that positrons are trapped at some defects in the oxide superconductors. In fact, perhaps because of this, the "bulk" lifetimes representing annihilation from the untrapped positron Bloch states are not yet established to any great degree of precision and reproducibility. To illustrate, some experimental results for reported Bloch-state lifetimes are collected in Table I. When more than one lifetime component is observed, the trapping model[18] must be used to extract the Bloch-state lifetime τ_B. For Table I, we have quoted results where either it seemed clear that the trapping model analysis had been carried out or where only

TABLE I. Experimental values of the lifetimes of positrons in oxide superconductors. The bulk lifetime is denoted τ_B, the short lifetime by τ_1, and the corresponding intensity by I_1. Values near T_c and the changes $\Delta\tau = \tau(T \simeq 0) - \tau(T_c)$ on cooling to $T \simeq 0$, are given.

Sample	Ref.	τ_B (ps)	τ_1 (ps)	I_1 (%)	$\Delta\tau$ (ps)
$YBa_2Cu_3O_{6.0}$	14	180	139±7	65	0
$YBa_2Cu_3O_{6.8}$	14	167	139±7	70	
$YBa_2Cu_3O_{7.0}$	14	176		100	10
$YBa_2Cu_3O_{7.0}$	30	158–176	72–125	8–21	
$YBa_2Cu_3O_{7.0}$	31	190		100	−15
$La_{1.85}Sr_{0.15}CuO_4$	15	175		100	10
La_2CuO_4	25	177		100	

a single lifetime was found. The intensity I_1 of the short lifetime τ_1 is included and is listed as 100% where only a single lifetime was found. Where changes below T_c were reported, we give the value at or just above T_c and the change on cooling to $T \simeq 0$.

Table I shows that the experimental lifetimes are somewhat uncertain, and probably sample dependent. $YBa_2Cu_3O_{7-x}$ is the most extensively studied material, and seems to show considerable sample-dependent variations of the lifetimes. Those for $La_{2-x}Sr_xCuO_4$ are in close agreement, and one is for the insulator, while the other is for the superconductor. There are also lifetime measurements on the thallium-based compound, but we are unaware of any lifetime data on Bi 2:2:1:2. In summary, the observed behavior is complicated, and theoretical guidance as well as careful experimental work will be needed if the information contained in the positron data is to be extracted.

Some theoretical information is already available. Jensen, Nieminen, and Puska[19] and later Barathi, Sundar, and Hariharan[20] used the same procedure that has proved so successful for defects in metals to calculate positron states at defects in Y 1:2:3. We use the same methods of calculation here, and present results as well for two other classes of oxide superconductors, La 2:1:4 and Bi 2:2:1:2, in order to see what common features, differences, and trends emerge from examining a series. Reasonably good samples of these materials, which are relatively straightforward to handle, seem to be attainable. The bismuth-based compound has a modulated structure, but we consider only the periodic and stoichiometric $Bi_2Sr_2CaCu_2O_8$.

II. CALCULATIONS

The calculations reported here use the superposed neutral-atom electron densities and potentials, which have a long history of use in conventional metals. These were chosen for several reasons. One was that we wished to compare our results with those of the two existing calculations[19,20] of which we are aware. Both of these previous calculations were for some monovacancies in Y 1:2:3. A second reason for using these potentials was that they give reasonable agreement with reported experimental Bloch-state lifetimes and so seem a realistic choice for defect studies.

There are certainly objections that can be raised to this approximation to the electrostatic potentials and charge densities of the oxide superconductors. The parent insulators are clearly ionic, and most of their ionic character must survive the doping, which produces the metallic and superconducting phases. In addition, the model uses a positron-electron correlation potential and an annihilation rate enhancement expression that describe positrons in an interacting three-dimensional homogeneous electron gas (jellium), and need not describe the correlations in the oxides particularly well, even in the metallic phase. For semiconductors and insulators, various expressions for the correlation potential and lifetime enhancement have been used,[6–11] and those developed by Puska *et al.* seem particularly promising.[10] The oxide superconductors may resemble both insulators and largely two-dimensional metals in various local regions within the unit cell, and the electron response to local positive probes is not yet understood in any detail. The present and previous[19,20] positron-lifetime calculations for these materials are hopefully steps in that direction.

The positron ground states are calculated by solving the Schrödinger equation in the potential constructed by superposing the constituent atoms of the crystal, and the overlap of the positron with the electrons is used to calculate the lifetime. Momentum spectra could be produced similarly, but the primary use of high-resolution momentum spectroscopy is to measure the momentum spectra of the electrons in good-quality crystals where defect trapping is negligible, and electron-positron band-structure methods are better for that purpose.[16,21] Doppler broadening is commonly used in defect studies, but the low resolution and different definitions of the parameters among different laboratories make quantitative comparison with theory difficult. The lifetimes, both mean and multiple as extracted from the trapping model, are preferable for quantitative comparison of theory and experiment.

This procedure for calculating the positron states and binding energies for positrons trapped at defects is well established.[3,4,1] The Schrödinger equation is solved on a three-dimensional grid of points. The calculations pre-

sented here used the relaxation algorithm described by Puska and Nieminen.[4] For delocalized Bloch states in the undefected materials we use the computational cell $0 \leq x \leq a/2$, $0 \leq y \leq b/2$, and $0 \leq z \leq c/2$, where a, b, and c are the lattice parameters, and the boundary conditions are mirror symmetry at the faces. For bound states, $\psi(\vec{r}) \rightarrow 0$ is used on the faces of the computational cell that are not mirror planes. For weakly bound states it is necessary to use a larger computational cell to obtain accurate energy values, requiring either large arrays or a coarse mesh. In view of the uncertainties in the positron potential for these systems, and also the current shortage of experimental data on well-characterized samples for comparison, the calculations presented here were limited to at most $31 \times 31 \times 61$ points within and on the faces of the computational cell.

The positron potential

$$v(\mathbf{r}) = v_{\mathrm{el}}(\mathbf{r}) + v_{\mathrm{corr}}(\mathbf{r}) \tag{1}$$

consists of the electrostatic potential v_{el} of the surrounding atoms or ions and a positron-electron correlation term v_{corr}. The electrostatic potential is the superposition of the electrostatic potentials of the constituent (neutral) atoms, obtained from electron densities calculated in the local-density approximation using Ceperley-Alder form of the exchange-correlation potential. The positron-electron correlation potential v_{corr} used is a function only of the local electron density $n(\mathbf{r})$, which is obtained by superposing the atomic densities. Typically, 500–1000 atoms within about 15 a.u. of an irreducible $\frac{1}{8}$ of the unit cell are used to construct the electron density and potential within it, which are then used to build their periodic counterparts. The explicit form of v_{corr} is the fit of Boronski and Nieminen.[5] The zero of our positron potential (1), and hence of the energies reported in the tables of the following sections, corresponds to zero electrostatic potential and zero electron density (so $v_{\mathrm{corr}} = 0$)—that is, a positron outside the crystal in vacuum with no allowance for surface dipoles.

We have calculated the positron lifetime in two ways. One is the traditional procedure, using the Brandt-Reinhiemer formula[22] and enhancement factors of 1.5 for core and d electrons. This requires a division of the electron densities into valence, d, and core electrons, and our division is, as usual, somewhat arbitrary. We regarded the O $2s^2 2p^4$, Ca $4s^2$, Cu $4s^1$, Sr $5s^2$, Y $5s^2$, Ba $6s^2$, and La $6s^2$ as valence electrons, the Cu $3d^{10}$, Y $4d^1$, and La $5d^1$ as d electrons, and the rest as core electrons. (This latter distinction is, of course, irrelevant when the same enhancement factor is used for core and d electrons.) Our second way of calculating the lifetime is by using

$$\lambda = \int d^3r\, n_+(\mathbf{r})\, \Gamma(n(\mathbf{r})), \tag{2}$$

where n_+ is the positron density and n is the total electron density. For Γ, the parametrization of Boronski and Nieminen[5] was used. This is more convenient, and has been shown by Jensen[23] to give as good agreement with experiment for metals as the traditional procedure. We find that the two formulas agree within a few picoseconds in the oxide superconductors.

III. RESULTS

The results of our calculations are that some vacancies in the oxides bind positrons as strongly, by ~ 1 eV, as do vacancies in conventional metals, while other vacancies and substitutional defects either do not bind positrons at all or bind them only marginally in our calculations. In view of the uncertainties in the potential construction and the coarse meshes that we have used at this stage for such diffuse bound states, binding energies $E_B \sim 0.1$ eV must be regarded as inconclusive, as must a result of no binding at a similar defect. However, weak positron traps with binding energies $\sim k_B T$ are likely responsible for at least some of the complex temperature dependences observed in positron measurements, and are particularly important because of this. We identify the kinds of defect that give these marginal binding energies in the calculations as candidate sites for weak binding of positrons, although the final answer will have to come from experiment.

With these reservations, in the tables below we simply quote the numerical values obtained in these calculations on the mesh and within the computational cell cited in each case. This gives some indication of the numerical accuracy resulting from the tradeoff between cell size and mesh spacing. It is not intended to convey the impression that the potential, electron density, and correlation models are reliable to the accuracy given. The positron energies have converged to better than the 10-meV accuracy of the tables.

The more tightly bound positron states are fairly well localized within the vacancies, and the trapped-state lifetimes are significantly longer than those of the delocalized Bloch states, by several tens of picoseconds for $E_B \simeq 0.5$–1 eV. The weak binding traps cause only small lifetime changes, probably too small to be experimentally resolved. It would be interesting if they could be distinguished instead by their binding energies, obtained from measurements of the temperature dependence. We present two sets of positron lifetimes τ, one from the traditional Brandt-Reinhiemer calculation, and one from the all-electron parametrization of Boronski and Nieminen.[5] We prefer the conceptual and computational simplicity of the latter, and our discussion of the results will refer to them when specific values are needed. The comparison is included in the tables simply as further[23] evidence that the differences between the two are small.

After some experiments with the mesh spacings and, for bound states, the distance at which the wave function could be set to zero, we decided on the following procedure. A mesh spacing of about $0.1a \simeq 0.4$ Å seemed adequate, and allowed us to conveniently place the boundary 8–12 Å from the defect. If no binding was obtained, we then investigated the possibility that this was simply due

to the imposition of the bound-state boundary condition $\psi_+(\mathbf{r}) = 0$ at too small r, leading to too much kinetic energy, in the following way. The Bloch-state energy was recalculated on a coarser mesh. The defect calculation was then repeated with use of this mesh spacing so that the zero boundary condition could be applied at larger distances without excessively large numbers of mesh points. The reason for repeating both calculations on the coarser mesh is that numerical errors are presumably minimized by subtraction of energies (to give binding energies) obtained from calculations that use the same mesh spacings. The Bloch-state energies did change slightly between the two meshes, and the details for each set of calculations are listed in the tables in the following sections.

A. La 2:1:4

The positron Bloch state wave function in defect-free La 2:1:4 is shown in Fig. 1, and the results for vacancies in La 2:1:4 in Table II. In Table II, the dimensions of the computational cells are given as multiples of the lattice parameters. (For La 2:1:4 and Bi 2:2:1:2, $a = b$.) The results for the two computational cell sizes and mesh spacings show that the calculation of low binding energies takes some care and that at the meV level the final answers have to be experimental. If the computational cell is too small, the localization kinetic energy exceeds the binding energy, and no binding is obtained. For very large computational cells, the mesh spacing has to be fairly large, which induces errors indicated by the differences in the Bloch-state energies, although the subtraction of like from like should minimize the errors in the binding energies. Nevertheless, when binding energies of less than a few tenths of an electron volt are found in these calculations they must be interpreted only as possible indications of a weak-binding site, while the absence of trapping in the calculations does not rule out weak binding.

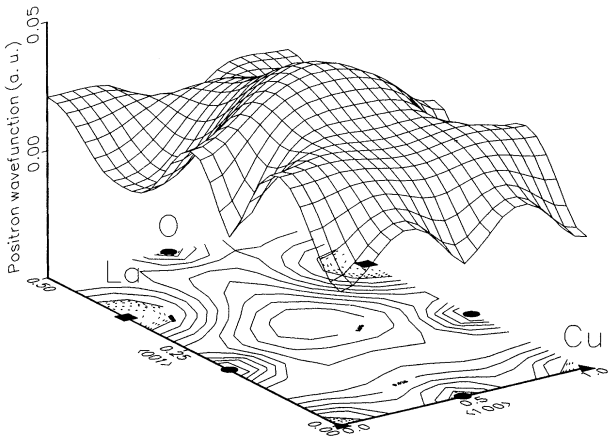

FIG. 1. The positron wave function for the delocalized Bloch state in La_2CuO_4. The contours are in steps of 0.001 (dashed lines) from 0.001 to 0.004 and steps of 0.005 (solid lines) from $0.005a_0^{-3/2}$ to $0.045a_0^{-3/2}$. The normalization is to one e^+ per unit cell.

The notation for the ions is that used by Pickett,[21] among others. The crystal structure used was that of Jorgensen *et al.*[24] The metal-ion vacancies bind positrons strongly, with binding energies $\sim$ 1 eV. The binding to oxygen vacancies is weak to nonexistent. Substitutional metal ions—the dopants—do not appear to bind positrons, at least in this model. We are led to conclude that, in La 2:1:4, any temperature dependence of the annihilation characteristics due to trapping should arise from weak binding to oxygen vacancies or possibly by diffusion to more extended defects like grain boundaries. This is in agreement with the observation by Wachs *et al.*[25] of only a single lifetime in La_2CuO_4 and negligible defect trapping at 300 K if there were few metal-ion vacancies and, in addition, either few oxygen vacancies

TABLE II. Calculated binding energies and lifetimes for positrons at defects in La_2CuO_4. Monovacancies are indicated by V, and substitutions as Sr (La) for a single La replaced by Sr. The size of the computational cell and the mesh within it are listed. Two calculated lifetime values are given. The one labeled τ_{BR} is calculated by the traditional Brandt-Reinhiemer formula with d and core electron contributions added, and τ_{BN} is calculated from the all-electron parametrization of Boronski and Nieminen.

Defect	Cell $a \times b \times c$	Mesh	E (eV)	E_B (eV)	τ_{BR} (ps)	τ_{BN} (ps)
Defect-free	0.5 × 0.5 × 0.5	11 × 11 × 31	3.43		138	135
Cu V	1.0 × 1.0 × 0.5	21 × 21 × 31	2.36	1.07	159	164
O(1) V (plane)	1.0 × 1.0 × 0.5	21 × 21 × 31	4.12			
O(2) V (apex)	1.0 × 1.0 × 1.0	21 × 21 × 61	3.61			
La V	1.0 × 1.0 × 1.0	21 × 21 × 61	−0.83	4.26	238	239
Sr (La)	1.0 × 1.0 × 1.0	21 × 21 × 61	4.12			
Defect-free	0.5 × 0.5 × 0.5	5 × 5 × 21	3.31		137	134
O(1) V (plane)	3.75 × 3.75 × 0.75	31 × 31 × 31	3.42			
O(2) V (apex)	3.75 × 3.75 × 1.5	31 × 31 × 61	3.25	0.06	164	157
Sr (La)	3.75 × 3.75 × 1.5	31 × 31 × 61	3.39			
Ba (La)	3.75 × 3.75 × 1.5	31 × 31 × 61	3.48			

or negligible binding to oxygen defects. Our calculated Bloch-state lifetime in the defect-free crystal (Table II) is shorter than the measured lifetime ("defect-free" in Table I), however. Temperature-dependent lifetime changes are reported in La 2:1:4, and the onset temperature appears indistinguishable from the superconducting T_c.[15]

B. Bi 2:2:1:2

Singh *et al.*[26] have calculated the positron wave function in Bi 2:2:1:2 using electrostatic potentials and charge densities obtained from linearized augmented-plane-wave electronic band-structure calculations along with the same e^+-e^- correlation potential as used here. Figure 2 presents our result for the Bloch-state wave function obtained in the superposed neutral-atom model for comparison. The positron density is greatest between the Bi-O planes at $z \simeq 0.2c$ and $0.3c$, and extends up toward the Cu-O plane at $z/c \simeq 0.45c$.

The results for vacancies in Bi 2:2:1:2 are shown in Table III. The structure used was that of Tarascon *et al.*[27] Positrons behave differently in this material. Aside from the large Bi, the metal-ion vacancies bind positrons only weakly or not at all, and we are unable to obtain any binding to oxygen defects. Any experimental temperature dependence associated with trapping at point defects will arise from weak binding to metal-ion vacancies. Figure 3 shows the positron wave function trapped at a Sr monovacancy, where it is bound by only ~ 0.1 eV. Unlike some of the more diffuse weakly bound states,[19] the positron is largely localized in the vicinity of the defect (possibly accounting for the relatively large lifetime change), but the wave function still extends up toward the Bi-O planes. $Bi_2Sr_2CaCu_2O_{8+x}$ has a complex modulated structure that accommodates the extra oxygens.

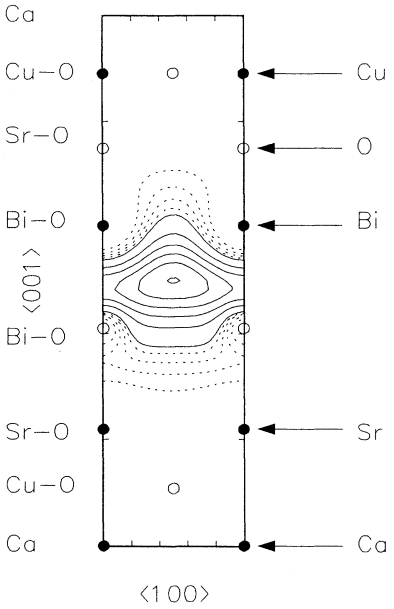

FIG. 2. The positron density of the delocalized Bloch state in $Bi_2Sr_2Ca_1Cu_2O_8$. The contours are in steps of 0.0001 (dashed lines) from 0.0001 to 0.0004, and steps of 0.0005 (solid lines) from 0.0005 to 0.003 e^+/a_0^3. The density is normalized to one e^+ per unit cell.

Dealing with such extended defects is computationally more difficult and is perhaps best postponed until the positron potential in these materials is better understood.

C. Y 1:2:3

The positron Bloch-state wave function in defect-free Y 1:2:3 that results from our positron potential is shown

TABLE III. Calculated binding energies and lifetimes for positrons at defects in $Bi_2Sr_2Ca_1Cu_2O_8$. The size of the computational cell and the mesh within it are listed. Two calculated lifetime values are given. The one labeled τ_{BR} is calculated by the traditional Brandt-Reinhiemer formula with d and core electron contributions added, and τ_{BN} is calculated from the all-electron parametrization of Boronski and Nieminen.

Vacancy	Cell $a \times b \times c$	Mesh	E (eV)	E_B (eV)	τ_{BR} (ps)	τ_{BN} (ps)
Defect-free	0.5 × 0.5 × 0.5	11 × 11 × 61	−1.61		180	183
Bi	1.0 × 1.0 × 0.5	21 × 21 × 61	−2.58	0.97	261	266
Sr	1.0 × 1.0 × 0.5	21 × 21 × 61	−1.70	0.09	234	238
Ca	1.0 × 1.0 × 0.5	21 × 21 × 61	−0.78			
Cu	1.0 × 1.0 × 0.5	21 × 21 × 61	−0.24			
O(1) (Cu plane)	1.0 × 1.0 × 0.5	21 × 21 × 61	−0.12			
O(2) (apex)	1.0 × 1.0 × 0.5	21 × 21 × 61	−0.51			
O(3) (Bi plane)	1.0 × 1.0 × 0.5	21 × 21 × 61	−1.09			
Defect-free	0.5 × 0.5 × 0.5	5 × 5 × 61	−1.66		179	183
Sr	3.75 × 3.75 × 0.5	31 × 31 × 61	−1.81	0.15	223	227
Ca	3.75 × 3.75 × 0.5	31 × 31 × 61	−1.57			
Cu	3.75 × 3.75 × 0.5	31 × 31 × 61	−1.29			
O(1) (Cu plane)	3.75 × 3.75 × 0.5	31 × 31 × 61	−1.17			
O(2) (apex)	3.75 × 3.75 × 0.5	31 × 31 × 61	−1.62			
O(3) (Bi plane)	3.75 × 3.75 × 0.5	31 × 31 × 61	−1.65			

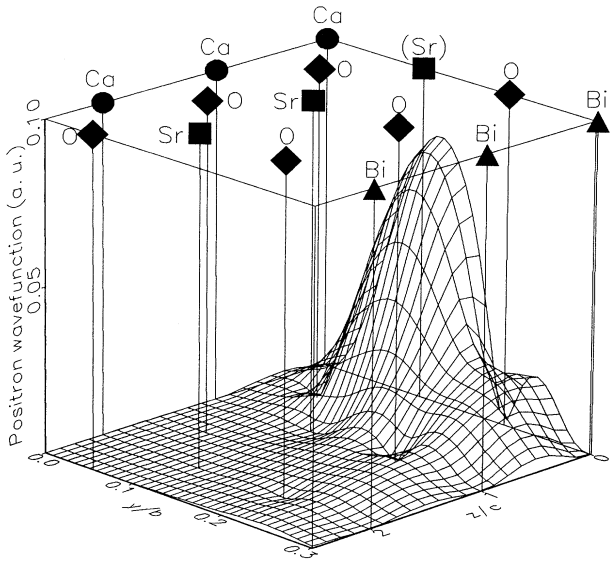

FIG. 3. The positron bound-state wave function at a Sr monovacancy in $Bi_2Sr_2Ca_1Cu_2O_8$. The normalization is to one e^+ in the sample. The atom positions on this y-z plane are indicated, and the Sr atom labeled (Sr) is the missing one.

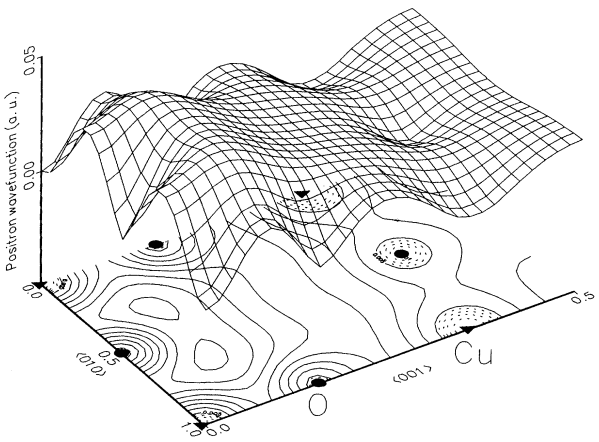

FIG. 4. The positron wave function for the delocalized Bloch state in $YBa_2Cu_3O_7$. The contours are in steps of 0.001 (dashed lines) from 0.001 to 0.004 and steps of 0.005 (solid lines) from $0.005a_0^{-3/2}$ to $0.04a_0^{-3/2}$. The normalization is to one e^+ per unit cell.

in Fig. 4. The results for vacancies in Y 1:2:3 are shown in Table IV. The structure used for Y 1:2:3 was that of Siegrist *et al.*[28] Positrons behave in this material more or less as in LSCO. The metal-ion vacancies trap positrons, and the binding energies are $\sim$ 1 eV, which is too large to contribute temperature dependence because of thermal detrapping. Instead, in Y 1:2:3 it is the oxygen-related defects that are the most likely candidates for weak-binding sites with $E_B \simeq k_BT$, and temperature dependence well above T_c is reported.[13] We conclude that in this material most of the experimental temperature dependence, except for that correlated with T_c, arises from weak binding to oxygen defects of various kinds.

The origin of this behavior, which makes Y 1:2:3 and La 2:1:4 quite different, at least in our calculations, from Bi 2:2:1:2, is illustrated by the difference in the positron Bloch-state energies in the perfect crystals. It is about 5 eV higher in La 2:1:4 and about 3.5 eV higher in Y 1:2:3 than in the more "open" Bi 2:2:1:2 structure. The more open structure makes more room available to the positron, and so it has less zero-point energy. Since the holes left by removing ions are about the same in the two compounds, the "bound state" at the smaller oxygen

TABLE IV. Calculated binding energies and lifetimes for positrons at defects in $YBa_2Cu_3O_7$. The size of the computational cell and the mesh within it are listed. Two calculated lifetime values are given. The one labeled τ_{BR} is calculated by the traditional Brandt-Reinhiemer formula with d and core electron contributions added, and τ_{BN} is calculated from the all-electron parametrization of Boronski and Nieminen. A crude approximation to a twin boundary, which is simply an O(1) vacancy at $(0, \frac{1}{2}, 0)$ and an O impurity added at $(\frac{1}{2}, 0, 0)$ is labelled "twin."

Vacancy	Cell $a \times b \times c$	Mesh	E (eV)	E_B (eV)	τ_{BR} (ps)	τ_{BN} (ps)
Defect-free	0.5 × 0.5 × 0.5	11 × 11 × 31	1.85		164	157
Cu(1)	1.0 × 1.0 × 0.5	21 × 21 × 31	0.91	0.94	197	200
Cu(2)	1.0 × 1.0 × 0.5	21 × 21 × 31	1.34	0.51	177	181
O(1) (chain)	1.0 × 1.0 × 0.5	21 × 21 × 31	2.13			
O(2) (plane a axis)	1.0 × 1.0 × 1.0	21 × 21 × 61	2.97			
O(3) (plane b axis)	1.0 × 1.0 × 1.0	21 × 21 × 61	2.97			
O(4) (apex)	1.0 × 1.0 × 1.0	21 × 21 × 61	2.45			
Defect-free	0.5 × 0.5 × 0.5	5 × 5 × 21	1.75		165	158
O(1) (chain)	3.75 × 3.75 × 0.75	31 × 31 × 31	1.69	0.06	181	170
O(2) (plane a axis)	3.75 × 3.75 × 1.5	31 × 31 × 61	1.85			
O(3) (plane b axis)	3.75 × 3.75 × 1.5	31 × 31 × 61	1.85			
O(4) (apex)	3.75 × 3.75 × 1.5	31 × 31 × 61	1.79			
Twin	3.75 × 3.75 × 0.75	31 × 31 × 31	1.74	0.01	189	177

vacancy lies above the bottom of the positron Bloch band in the more open structure, and those at the larger metal ion vacancies lie much closer to it.

IV. THERMAL DETRAPPING

The assortment of possible weak-binding sites found in the calculations makes it plausible that such sites do exist in the oxides, and a simple model can be used to illustrate the temperature dependence of the mean positron lifetime that might be observed if weak-binding sites existed. Our calculations indicate that the lifetime of positrons trapped at those sites is likely only slightly longer than that of the untrapped positrons, and the two lifetimes may not be experimentally resolvable.

The model is the two-state trapping model discussed by Bergersen and Stott,[18] in which the positrons can be in either free states (f) or trapped states (t). Detailed balance establishes the relation between the rates w for trapping and detrapping, which is conveniently written

$$w_{t\to f} = D(T)\, w_{f\to t}, \tag{3}$$

where D is a temperature-dependent "detrapping ratio," and the trapping rate $w_{f\to t}$ will be supposed independent of temperature. If the density of untrapped states has the $\varepsilon^{1/2}$ three-dimensional free-particle form, the temperature dependence of D is

$$D(T) = D_0 \left(\frac{k_B T}{E_B}\right)^{3/2} e^{-E_B/k_B T}, \tag{4}$$

where E_B is the binding energy[29]. The prefactor

$$D_0 = \frac{(m^*/m_e)^{3/2}}{g_t a_0^3} \left(\frac{E_B}{4\pi\ \mathrm{Ry}}\right)^{3/2} \tag{5}$$

can be of order unity if, for example, the positron effective mass m^* is the electron mass m_e, the binding energy is 300 K, and the volume trap density g_t corresponds to $\sim 5 \times 10^{-5}$ per cell of Y 1:2:3. We do not yet have estimates of m^* or the positron mobility, however.

Solving the rate equations for the trapping model gives the mean lifetime[18]

$$\overline{\tau} = \tau_f \frac{1 + \tau_t w_{f\to t}[1 + D(T)]}{1 + \tau_t w_{f\to t}[\tau_f/\tau_t + D(T)]}, \tag{6}$$

where τ_f and τ_t are the two lifetimes. As an illustration, Fig. 5 shows the mean lifetime that results when τ_t is 10% longer than τ_f and the prefactor of (4) has the values 1 or 10, which label the two curves shown. The larger prefactor sharpens the crossover from 50% trapping (for $w_{f\to t} = 1/\tau_f$) at low temperature to essentially all positrons untrapped at high temperature. This crossover occurs at $T \sim E_B/k_B$.

V. DISCUSSION

We were interested in studying a series of oxides to see if there were common features and trends in the positron characteristics. The trends that have appeared are related to crowding and ion size. The materials that we chose for study here were $La_{2-x}(Sr,Ba)_xCuO_4$ with $T_c \simeq 40$ K, $Bi_2Sr_2CaCu_2O_{8+x}$ with a $T_c \simeq 85$ K, and $YBa_2Cu_3O_{7-x}$ with a $T_c \simeq 90$ K. As viewed by a positron, La 2:1:4 and Y 1:2:3 are noticeably the more crowded, and positrons are firmly squeezed out of the bulk and into the larger metal-ion defects. The ion sizes as seen by a positron are roughly indicated by the extent of the electrostatic potential in the 1-eV range of the positron zero-point energy, and these are compared in Fig. 6 for the ions comprising Y 1:2:3. These potentials are superposed and then the positron-electron correlation potential v_{corr} is added, which results in a nonpairwise

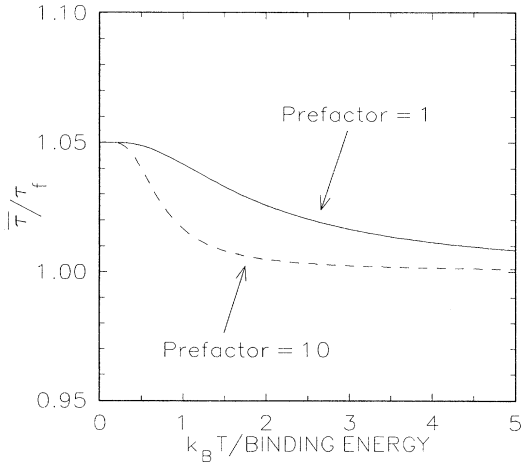

FIG. 5. An illustration of the effects of positron thermal detrapping from a weakly bound state. The trapping rate $w_{f\to t}$ is equal to the annihilation rate τ_f^{-1} of untrapped positrons, and the lifetime of the trapped state τ_t is 10% longer than τ_f.

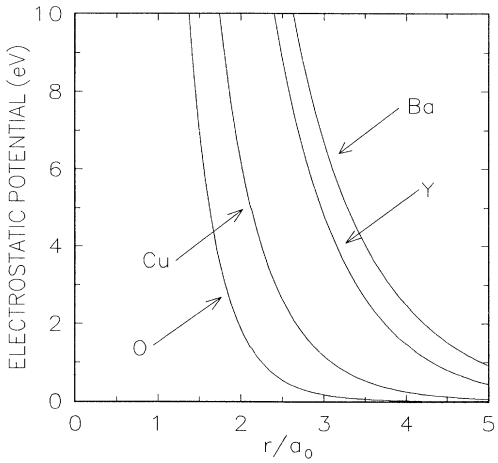

FIG. 6. Comparison of the electrostatic potentials of the isolated neutral atoms Ba, Y, Cu, and O.

positron-atom interaction. Nevertheless, Fig. 6 remains a reasonable guide. Oxygen is the smallest atom present, and so removing oxygen leaves the smallest hole, and a trapped positron has a high zero-point kinetic energy. The Bi-based compound is different. In Bi 2:2:1:2, metal vacancies give only weak binding, and positrons do not trap at oxygen vacancies. The explanation seems to be the following. The perfect crystal structure, as viewed by a positron in its ground state, provides more open space, and the ground-state energy (the bottom of the positron band) is lower. A copper vacancy looks about the same here as in La 2:1:4 or Y 1:2:3, but as a consquence of the lower band bottom, binding does not occur.

The neutral-atom potentials used in these calculations were chosen in part so that the results would be directly comparable with those of the two existing calculations[19,20] of which we are aware, both of which were for some monovacancies in Y 1:2:3. Where they overlap, our results are in fairly close agreement with those of Jensen, Nieminen, and Puska,[19] and the differences probably reflect uncertainties due to the mesh spacings used. Our results differ in a number of respects from those of Bharathi, Sundar, and Harihan.[20]

A second reason for using these potentials was that they gave reasonable agreement with reported experimental Bloch-state lifetimes, and so seem a realistic choice for defect studies. So far, since defected samples are not particularly well characterized (with the possible exception of a twin-boundary study[30]), the only comparison with experiment that can be made to test the validity of calculations is with the measured Bloch-state lifetimes. Table I showed that the experimental lifetimes are somewhat uncertain, and probably sample dependent. Our calculated Bloch-state lifetime in $YBa_2Cu_3O_7$ is close to the lower limit of the range of observations. That for La_2CuO_4 is considerably shorter than the two reported results, one of which is for the insulator and one for the superconductor, and these two experimental values are in close agreement. This is evidence for the difficulties, referred to in Sec. II, with the positron-electron correlation expressions that lead to problems with the potential or lifetime expressions for this class of materials. The fractional changes in lifetime on trapping, which are of the most interest, are expected to be more reliable than the absolute magnitudes.

The question of the positron-electron correlation potentials and rate enhancements suitable for these unusual systems remains an interesting one. It will no doubt require both experimental and theoretical efforts to refine these to the degree that has been accomplished for conventional metals. The oxide superconductors are largely ionic and highly anisotropic metals in which the electron correlations are probably strong. They have closely related insulating parents with which comparisons can be made. If the understanding of positron properties in these materials can be developed to the extent that has been done for conventional metals, positron annihilation may become a useful materials-characterization tool on these materials just as it certainly has become for conventional metals. A purpose of the initial catalog of defect-trapping characteristics presented here is to assist and encourage that development. The other important reason for furthering the understanding of defect trapping is the hope of untangling this complication from experiments that confirm that there indeed are changes in annihilation characteristics caused by the onset of superconductivity, and which establish the changes in charge distribution and response that accompany oxide superconductivity.

ACKNOWLEDGMENTS

The support of this work by the Electric Power Research Institute and by the Virginia Center for Innovative Technology is gratefully acknowledged.

[1] M. J. Puska, Phys. Status Solidi A **102**, 11 (1987).
[2] P. J. Shultz and K. G. Lynn, Rev. Mod. Phys **60**, 701 (1988).
[3] M. J. Puska and R. M. Nieminen, J. Phys. F **13**, 333 (1983).
[4] M. J. Puska and R. M. Nieminen, Phys. Rev. B **29**, 5382 (1984).
[5] E. Boronski and R. M. Nieminen, Phys. Rev. B **34**, 3820 (1986).
[6] S. Dannefaer, P. Mascher, and D. Kerr, Phys. Rev. Lett. **56**, 2195 (1986).
[7] M. J. Puska, O. Jepsen, O. Gunnarsson, and R. M. Nieminen, Phys. Rev. B **34**, 2695 (1986).
[8] P. J. Schultz, E. Tandberg, K. G. Lynn, B. Nielsen, T. E. Jackman, M. W. Denhoff, and G. C. Aers, Phys. Rev. Lett. **61**, 187 (1988).
[9] M. J. Puska and C. Corbel, Phys. Rev. B **38**, 9874 (1988).
[10] M. J. Puska, S. Mäkinen, M. Manninen, and R. M. Nieminen, Phys. Rev. B **39**, 7666 (1989).
[11] S. Mäkinen and M. J. Puska, Phys. Rev. B **40**, 12 523 (1989).
[12] Y. C. Jean, S. Wang, H. Nakanishi, W. N. Hardy, M. E. Hayden, R. F. Kiefl, R. L. Meng, H. P. Hor, J. Z. Huang and C. W. Chu, Phys. Rev. B **36**, 3994 (1987).
[13] S. G. Usmar, P. Sferlazzo, K. G. Lynn, and A. R. Moodenbaugh, Phys. Rev. B **36**, 8854 (1987).
[14] D. R. Harshman L. F. Schneemeyer, J. V. Waszczak, Y. C. Jean, M. J. Fluss, R. H. Howell, and A. L. Wachs, Phys. Rev. B **38**, 848 (1988).
[15] Y. C. Jean, J. Kyle, H. Nakanishi, P. E. A. Turchi, R. H. Howell, A. L. Wachs, M. J. Fluss, R. L. Meng, H. P. Hor, Z. J. Huang, and C. W. Chu, Phys. Rev. Lett. **60**, 1069 (1988); see also D. R. Harshman, L. F. Schneemeyer, and J. V. Waszczak, Phys. Rev. Lett. **61**, 2003 (1988).
[16] E. C. von Stetten, S. Berko, X. S. Li, R. R. Lee, J. Bryn-

stad, D. Singh, H. Krakauer, W. E. Pickett, and R. E. Cohen, Phys. Rev. Lett. **60**, 2198 (1988).
[17]M. Manninen and R. M. Nieminen, Appl. Phys. A **13**, 93 (1981).
[18]B. Bergersen and M. J. Stott, Solid State Commun. **7**, 1203 (1969).
[19]K. O. Jensen, R. M. Nieminen, and M. J. Puska, J. Phys. Condens. Matter **1**, 3727 (1989).
[20]A. Bharathi, C. S. Sundar, and Y. Hariharan, J. Phys. Condens. Matter **1**, 1467 (1989).
[21]W. Pickett, Rev. Mod. Phys. **61**, 433 (1989).
[22]W. Brandt and J. Reinhiemer, Phys. Lett. **35A**, 109, (1971).
[23]K. O. Jensen, J. Phys. Condens. Matter **1**, 10 595 (1989).
[24]J. D. Jorgensen, H.-B. Schüttler, D. G. Hinks, D. W. Capone, K. Zhang, M. B. Brodsky, and D. J. Scalapino, Phys. Rev. Lett. **58**, 1024 (1987).
[25]A. L. Wachs, P. E. A. Turchi, Y. C. Jean, K. H. Wetzler, R. H. Howell, M. J. Fluss, D. R. Harshman, J. P. Remeika, A. S. Cooper, and R. M. Fleming, Phys. Rev. B **38**, 913 (1988).
[26]D. Singh, W. E. Pickett R. E. Cohen, H. Krakauer, and S. Berko, Phys. Rev. B **39**, 9667 (1989).
[27]J. M. Tarascon, Y. LePage, P. Barboux, B. G. Bagley, L. H. Greene, W. R. McKinnon, G. W. Hull, M. Giroud, and D. M. Huang, Phys. Rev. B **37**, 9382 (1988).
[28]T. Siegrist, S. Sunshine, D. W. Murphy, R. J. Cava, and S. M. Zahurak, Phys. Rev. B **35**, 7137 (1987).
[29]Manninen and Nieminen, Ref. 17, give this expression along with an extensive discussion of the thermal detrapping of positrons in other contexts as well.
[30]S. G. Usmar, K. G. Lynn, A. R. Moodenbaugh, M. Suenaga, and R. L. Sabatini, Phys. Rev. B **38**, 5126 (1988).
[31]Y. C. Jean, C. S. Sundar, A. Bharathi, J. Kyle, H. Nakanishi, P. K. Tseng, P. H. Hor, R. L. Meng, Z. J. Huang, C. W. Chu, Z. Z. Wang, P. E. A. Turchi, R. H. Howell, A. L. Wachs, and M. J. Fluss, Phys. Rev. Lett. **64**, 1593 (1990).